

Analysis of Turbulence Profiles from Three Tall Towers: Departure from Similarity Theory in Near-Neutral and Stable Conditions

Brent M. Bowen*

Environmental Protection Department, Lawrence Livermore National Laboratory, Livermore, California, USA

Abstract: Long-term wind and turbulence profiles were analyzed for all stability conditions at three tall, multi-level towers located at the Los Alamos National Laboratory (LANL), Rocky Flats Environmental Plant (RF), and the Boulder Atmospheric Observatory (BAO). The LANL and RF sites are located in complex terrain and the BAO is located over relatively simple terrain, but within 3 to 5 km of an abrupt 20 to 30 m increase in terrain. Results indicate that normalized turbulence parameter profiles at all three sites agree well with widely used empirical relationships during unstable conditions.

During near neutral conditions, σ_u parameter profiles are also well behaved at all three sites while σ_w increases with height for complex fetch (BAO downwind of bluff, LANL, and RF) while σ_w remains nearly constant up to 200 m AGL at BAO with simple fetch. The σ_w/u_* values at 10-m AGL are close to one at all sites and they increase by an order of 50% in the lowest 60 to 200 m for complex fetch and remain approximately constant in the lowest 200 m with simple fetch.

During very stable conditions, typical values of σ_u and σ_v range between 0.4 to 0.6 ms^{-1} and increase slightly with height while median σ_w values nearly double from about 0.1 to 0.2 ms^{-1} between the 10- and 100 to 200-m levels. A comparison of predicted with measured u_* values at two of the sites shows generally good agreement over 6 stability categories. It is suggested that M-O similarity theory will usually greatly underestimate vertical diffusivity and dispersion during very stable conditions, especially at larger heights, based on idealized Kz profiles calculated from measured σ_w values. Finally, rules of thumb are formulated to describe departure from similarity theory during near-neutral and stable conditions.

Keywords: Turbulence, towers, similarity.

1. INTRODUCTION

Atmospheric dispersion models require accurate turbulence estimates in order to reliably characterize downwind dispersion and atmospheric pollutant concentrations. While simple Gaussian dispersion models often use Pasquill-Gifford-Turner dispersion coefficients to estimate downwind dispersion, the use of Monin-Obukhov similarity theory with near surface wind speed (u), estimated roughness length (z_0), mixing layer height (h), and experimentally derived factors can reliably characterize three-dimensional downwind dispersion over various kinds of terrain. Even when turbulence parameters are measured at standard tower height (~ 10 m), the turbulence parameter profile must be estimated throughout the surface layer using, for example, the power law recommended by the U.S. Environmental Protection Agency [1].

The use of widely used turbulence relationships is often inappropriate since they are based on a limited number of field experiments, conducted primarily over flat, smooth, and uniform (FSU) terrain. Hicks [2] points out: "The extensive

field studies of the 1960s and 1970s should offer no great solace, since the sites were carefully chosen as outdoor laboratories to test similarity and its consequences in fitting circumstances. There was no test of similarity in conditions that violated the assumptions of similarity."

Several later field studies provided insight on the effect of complex terrain on downwind turbulence and dispersion. Panofsky *et al.* [3] first suggested that rolling terrain enhanced the wind direction standard deviation, σ_θ . Their findings indicate that σ_θ typically increases by 150% to the lee of a low mountain and by 40% in slightly rolling terrain compared to flat terrain. Hanna [4] demonstrates in another field study that σ_θ is typically 60% larger in a river valley for cross-valley flow, likely a result of upwind terrain irregularities. The same study also suggests that irregular terrain causes the horizontal dispersion parameter, σ_y , to increase by an even greater amount. Ludwig and Dabberdt [5] show that σ_θ increases by 10% to 85% downwind of downtown St. Louis versus more rural upwind fetch. Tieleman [6] points out that peak wavelengths of horizontal turbulence components caused by complex terrain can require several kilometers of fetch to dissipate and adjust to the 'local' terrain. However, this study as well as those by Panofsky *et al.* [3] and other applied researchers have generally dismissed

*Address correspondence to this author at the Environmental Protection Department, Lawrence Livermore National Laboratory, Livermore, California, USA; E-mail: bbowen@yahoo.com

the effect of terrain features on vertical turbulence and assume that the higher frequency vertical turbulence quickly adjusts to local terrain.

The neglect of terrain-enhanced vertical turbulence may actually have occurred because many field experiments have taken place in homogenous terrain and σ_w profiles have typically been limited to about 25 m AGL or less [7]. Beljaars *et al.* [8] demonstrate in a flat agricultural area (Cabauw tower) that measured σ_w and friction velocity (u_*) both increase 40% with increasing height above ground from 3.5 to 22.5 m with non-uniform fetch and they remain unchanged with uniform fetch. Later studies by Bowen [9, 10] indicate that during near-neutral conditions with wind speed (u) of 5 to 6 ms^{-1} , σ_w increases by about 0.3 ms^{-1} in the lowest 100 meters at the three sites investigated in this study: a 'locally' smooth site surrounded by rolling terrain, a forested site with canyons, and at a site 4 km downwind of a 20- to 30-m high bluff. All of these studies indicate that while σ_w increases with height, the standard deviations of longitudinal (σ_u) and lateral (σ_v) wind speed are nearly constant with height in heterogeneous terrain. Terrain has increasingly less influence on turbulence, as conditions become more unstable.

The stable boundary layer (SBL) presents challenges to estimate turbulence in all terrain. Hanna and Chang [11] point out that horizontal meandering motions near the surface are always present during stable conditions at all types of field sites and they therefore recommend a minimum σ_v value of 0.5 ms^{-1} over one-hour averaging times. Enhanced vertical turbulence in the SBL is less understood yet potentially more important in downwind dispersion. Field studies at Savannah River Laboratory [12] and Rocky Flats [13] demonstrate how the combination of strong wind direction shear and enhanced vertical turbulence in the lowest hundreds of meters can influence vertical and horizontal transport of surface tracer material. This results in broader plumes and secondary plumes inconsistent with near-surface wind direction. The formation of a nocturnal, low-level jet is suggested to enhance σ_w in the 100-500 m AGL level (and causes larger ground-level pollutant concentrations from medium and tall stacks), especially after 10:00 p.m. LT according to Hanna and Chang [11]. These studies and others suggest that enhanced σ_w in the SBL can lead to much stronger vertical diffusivity than indicated by M-O similarity theory and yield plume transport errors during times with strong horizontal wind direction shear.

Long-term wind and turbulence profiles up to 200 m AGL and u_* are analyzed in this study for all stability conditions at three tall, multi-level towers located in the western U.S. The Los Alamos National Laboratory (LANL) and Rocky Flats Environmental Technology (RF) sites are located in complex terrain and the Boulder Atmospheric Observatory (BAO) is located over relatively simple terrain, but within 3 to 5 km of an abrupt 20 to 30 m increase in terrain. Profiles of median, 15-minute averaged turbulence parameters (σ_u , σ_v , and σ_w), standard deviations of horizontal and vertical wind angle fluctuations (σ_θ and σ_ϕ), and winds are analyzed for eight wind direction sectors at the three towers. Predicted u_* at BAO and LANL are compared to measured values at both sites. Finally, differences between widely used Kz profiles based on similarity theory and profiles estimated using measured σ_w during stable conditions, and their possible effect on model results, are discussed.

2. DESCRIPTION OF SITES AND INSTRUMENTATION

The three tower sites used in this study are located over various types of terrain with semiarid climate (see Table 1). The RF and BAO sites are located east of the Front Range in east-central Colorado and LANL is located in north-central New Mexico. The site elevations range from 1575 MSL at BAO to 2250 MSL at LANL. The fetch is complex at RF and LANL with sharp terrain changes of up to 50 and 100 m caused by drainage areas and canyons, respectively [9]. The vegetation is sparse at RF while ponderosa trees are widespread at LANL. The local terrain at BAO is simple, located in slightly rolling farmland with ground cover of wheat or wheat stubble with 0.25 to 0.5 m height [14]. The low relief, with slopes of 20 m km^{-1} or less, extends at least 10 km to the north, east, and south of this site. However, a 20 to 30-m bluff extends approximately 3.5 km to the west and 4 to 5 km to the northwest and southwest of the tower.

All towers are guyed with open lattice structures of galvanized steel. Booms are used to support the tower instruments. While towers at RF and LANL are instrumented to take routine operational measurements, the BAO was equipped with various sensors from late March through early June of 1995 as part of the Ground-Based Remote Sensor Characterization study [15]. Note that the data measured at the 300-m level were affected by electrical interference and therefore were not analyzed in this study.

Wind direction and speed were measured by low-threshold cup and vane systems at RF and by low threshold propeller anemometers at LANL. Propellers with an extender

Table 1. Site Characteristics of the Three Towers Used in this Study

Site	Period of Record	z_0 (cm)	Tower Heights (m)	Fetch	Comments
RF	1 year	2.5-8	10, 25, 60	Rolling terrain with .5m-high grass	Site on 2.0° sloping bench
LANL	1 year	40-90	12, 23, 46, 92	Canyons 50-100 m deep and 100-200 m wide; 20-m-high ponderosa pines	Site on 2.5° sloping plateau
BAO	10 weeks	0.6-34	10, 50, 100, 200	Gently rolling with .25-.5 m wheat/wheat stubble	20-30 m bluff located 3.5-5 km toward SW-NW

and medium weight blades measured vertical velocity at both of these sites. Sonic anemometers provided the wind direction and speed and vertical velocity at BAO. Thermistors located at multiple levels provided temperature data at all sites. The data were sampled at a 1 Hz rate at RF and LANL and a 10 Hz rate at BAO. Dataloggers at all towers provided 15-minute averages. Momentum flux, based on eddy correlation of measured horizontal and vertical wind fluctuations, was used to calculate u_* at LANL and BAO.

3. DATA ANALYSIS DESCRIPTION

Fifteen-minute averaged wind, turbulence, and momentum flux data were analyzed for eight directional sectors (45° wide) and 6 stability categories, defined by 6 ranges of Richardson number (Ri) values. The 15-minute averaging period is a good compromise since a shorter period may be inadequate to characterize turbulence while wind direction changes or “meandering” will become more important for longer averaging periods such as an hour, especially during stable conditions. These ranges correspond roughly to Pasquill stability categories defined according to a method suggested by Sedefian and Bennett [16] based on the Businger [17] formulation. The Ri values, detailed in section 4, are calculated using 15-minute averages of u and potential temperature (θ) values at the two lowest heights of the towers for each site and sector:

$$Ri = g/T (\Delta\theta/\Delta z)/(\Delta u/\Delta z)^2, \quad (1)$$

where g is the acceleration of gravity and T is the average temperature. Note that the bottom and top of the layers (i.e., the two lowest measurement levels) used to calculate Ri are 10-25, 11-23, and 10-50 m at the RF, LANL, and BAO towers, respectively.

The z_o value was calculated from measured σ_u and u at 10- to 12-m heights for each site sector during more strictly-defined near-neutral stability by the following expression suggested by Tieleman [6] and others:

$$z_o = \exp[\ln z - 1/(\sigma_u/u)] \quad (2)$$

Nighttime cases with 10- to 12-m u greater than 5 ms^{-1} and daytime cases with u greater than 5 ms^{-1} with slight insolation and with u greater than 6 ms^{-1} with moderate insolation are defined as near neutral. Slight and moderate insolation ranges are defined as 70-350 and 350-700 Wm^2 , respectively, and a value of 70 Wm^2 is used to define day and night. Equation (2) is derived from the logarithmic wind profile equation and the widely used approximation $\sigma_u/u_* = 2.5$ based on measurements over flat and smooth terrain.

The u_* values are estimated at all sites using the following relationship suggested by Holtslag and Van Ulden [18] based on integrated flux-profile relationships of Dyer and Hicks [19, 20]:

$$u_* = kU_Z [\ln(z/z_o) - \psi_M(z/L) + \psi_M(z_o/L)]^{-1}, \quad (3)$$

where k is the von Karman constant (0.41), U_Z is the wind speed (ms^{-1}) at a specific height, L is the Monin-Obukhov length (m) and ψ_M is a function of the dimensionless wind gradient, ϕ_m .

The L is estimated from the calculated Ri using the following relationships:

$$z/L = Ri \text{ for } Ri < 0$$

$$z/L = Ri/(1 - 5Ri), \text{ for } 0 \leq Ri < 0.2 \quad (4)$$

Arya [21] points out that the second relationship of Eq. (4) implies a critical value of $Ri \approx 0.2$, although similarity theory is not expected to remain valid in extremely stable conditions. Therefore, a maximum L value of 12 (RF and BAO) and 17 (LANL) is assumed based on relationships suggested by Golder [22]. The u_* was calculated from winds at 10-m heights at BAO and RF and the 12-m height at LANL. Note that z_o is calculated using σ_u in Equation (2) with the u_* representing a regional value affected by more distant upwind terrain instead of a local value where z_o is calculated from wind speed profiles. Verkaik and Holstag [23] point out that meteorological masts are often placed in sites with undisturbed terrain and therefore local roughness is usually smaller than the large-scale roughness.

Several empirical studies at tall towers indicate that surface layer theory is typically valid up to heights of 80-m in all stabilities [24] and at least 150 m during windy, near-neutral conditions [25] at sites with homogeneous and relatively flat terrain. Gryning *et al.* [24] also point out that departure from surface layer theory gradually increases above the surface layer up to a 300-m height. Therefore measurements from most if not all tower levels in this study are expected to be within or slightly outside the surface layer in unstable and near-neutral conditions. However, some or all tower levels are probably above the surface layer and occasionally above the boundary layer during stable conditions.

Median wind speeds, turbulence parameters, and u_* were calculated in this study. Median values are better able to describe ‘typical’ conditions than mean values since they give less weight to extreme data (e.g., very strong winds).

4. RESULTS AND DISCUSSION

4.1. Ri-Based Stability Category Distribution At Tower Sites

The distribution of stability categories based on Ri range was calculated for 4 fetches and is shown in Fig. (1). Typical Ri values of the class limits are also shown. Note that both BAO fetches experience somewhat more neutral and near-neutral conditions than the LANL and RF towers during the respective study periods. Some of the differences are probably attributed to the limited study period at BAO (i.e., during relatively breezy spring). The greater frequency of unstable conditions for simple compared to complex fetch at BAO results from diurnal wind direction change. Finally, persistent nocturnal drainage winds contribute to the very high frequency of F stability at both LANL and RF.

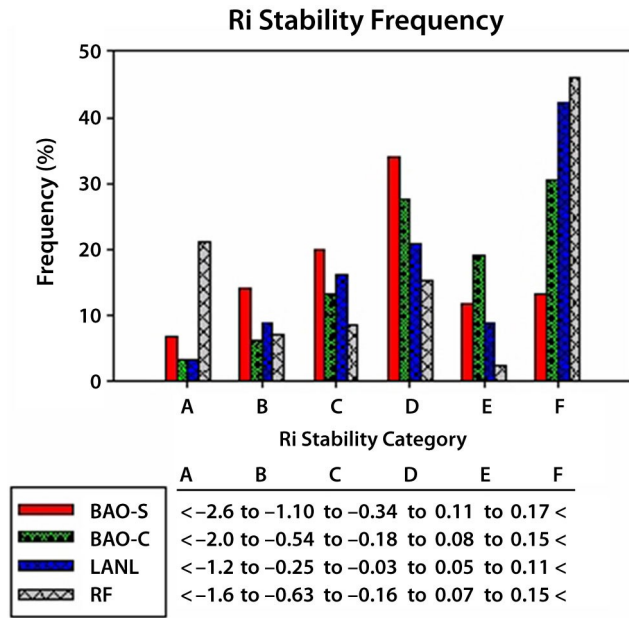


Fig. (1). Frequency distribution of stability categories based on Ri for 4 fetches at 3 sites. Class limits for each stability category transition are shown for each fetch. The simple and complex fetches at BAO are denoted as -S and -C, respectively.

4.2. Normalized Turbulence Parameter Profiles by Stability

Profiles of normalized turbulence parameters were calculated for all Ri classes and are shown in Figs. (2-7). Although turbulence parameter values varied across individual directional sectors, the normalized values were more constant and therefore averaged across sectors. Note that σ_w is more appropriately scaled by w_* for the most unstable conditions and larger heights; however, u_* values were used throughout for ease of comparisons and because the boundary layer depths were unavailable in order to calculate w_* . The σ_u/u_* values for A are at or somewhat below an expected range of 3.3 to 4.8 based on equations suggested by Panofsky *et al.* [26] using ranges of h and L between 1 and 2 km and 10 to 20 m, respectively. The σ_v/u_* values are somewhat larger than σ_u/u_* values and are within the previously mentioned expected range, although they decrease with height. The σ_w/u_* values increase sharply with height as expected for all fetches at approximately the same rate. The σ_w/u_* values at BAO and LANL agree reasonably well with predicted ranges of approximately 1.75 to 2 and 3.25 to 3.75 at the 10- and 100-m AGL levels, respectively. The values at RF are considerably less than at the other sites. The combination of relatively smooth terrain and light winds during unstable conditions allows occasional stalling of the vertical propeller at RF, thereby reducing the mean σ_w/u_* values.

The normalized turbulence parameter profiles show slight changes for the B stability class (Fig. 3). The most important change during B stability is that σ_v/u_* profiles at

all fetches converge to between values of 3.0 to 3.6. The σ_u/u_* and σ_v/u_* values for B stability nearly agree, except at RF. The σ_v/u_* continues to decrease slightly with height. The σ_w/u_* profiles show only minor changes from those in A stability.

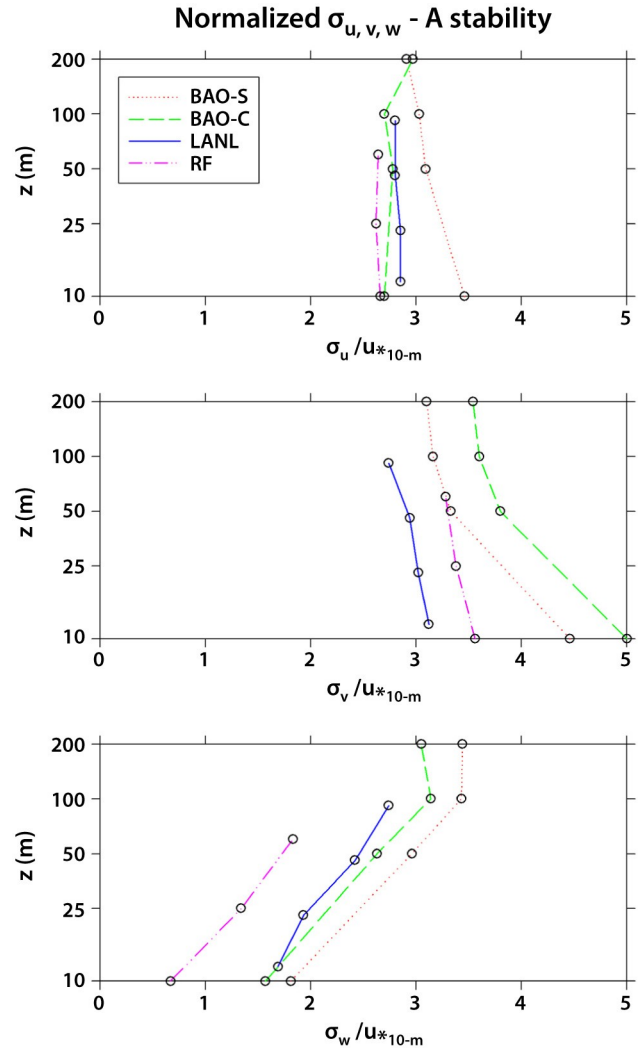


Fig. (2). Normalized turbulence parameter ($\sigma_{u,v,w}/u_*$) profiles for 4 fetches at 3 sites during A stability.

Normalized turbulence coefficient values decrease as stability approaches neutral (see Fig. 4). Both σ_u/u_* and σ_v/u_* values range from about 2.5 to slightly above 3 for C stability and are generally constant with height. The σ_w/u_* values have decreased considerably from the transition to C stability, especially at higher heights. Note that the rate of increase with height of σ_w/u_* has decreased as well. The σ_w/u_* profiles from all 4 fetches now show very good agreement.

The normalized turbulence coefficients decrease further in near-neutral conditions and remain nearly constant with

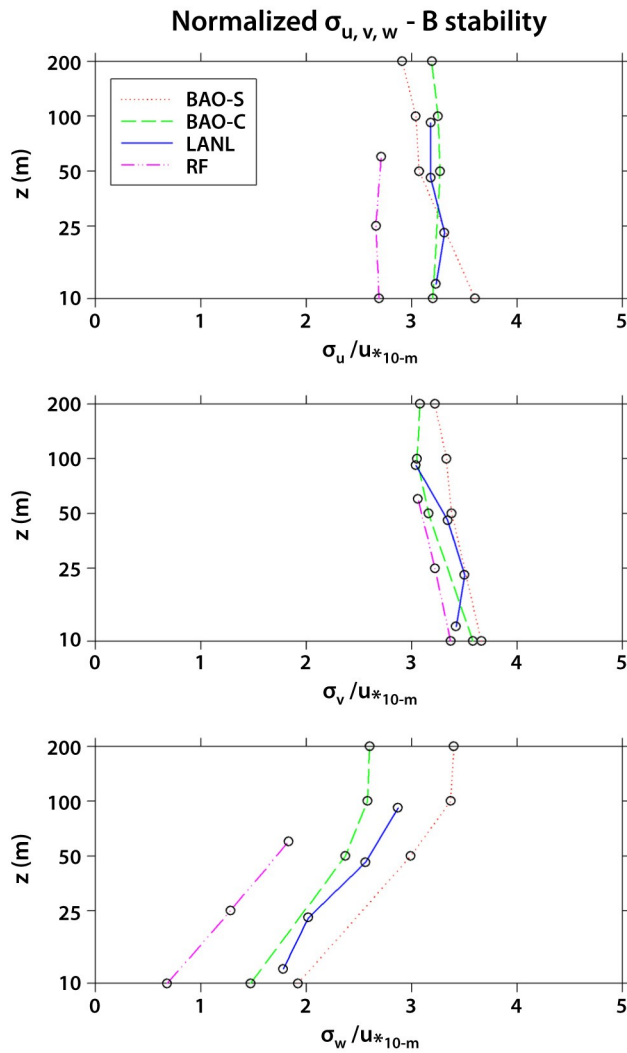


Fig. (3). Same as Fig. (2), except during B stability.

height (see Fig. 5). It is not surprising that lowest-level σ_u/u_* values at all fetches converge closely to the expected value of 2.5, since z_o was estimated at all sites assuming the same ratio (the use of Eq. 2). The σ_v/u_* values are only slightly less than σ_u/u_* values, generally equaling or slightly exceeding the widely used ratio of 2. The median σ_w/u_* values at 10 to 12 m AGL are close to one when averaged over all fetches. However, the shapes of the profiles differ according to fetch. The σ_w/u_* profile at BAO with simple fetch indicates little change with height, thereby agreeing with M-O similarity theory. The three σ_w/u_* profiles with complex fetch all indicate an increase with height and therefore depart from similarity theory. Since the number of near-neutral conditions is nearly equal between day and night, and because σ_w nighttime analyses indicate similar results, it is doubtful that convection skews these results.

The σ_u/u_* and σ_v/u_* profiles for E stability indicate a slight increase and more variation among fetches compared to D stability (see Fig. 6). Also note that the values are

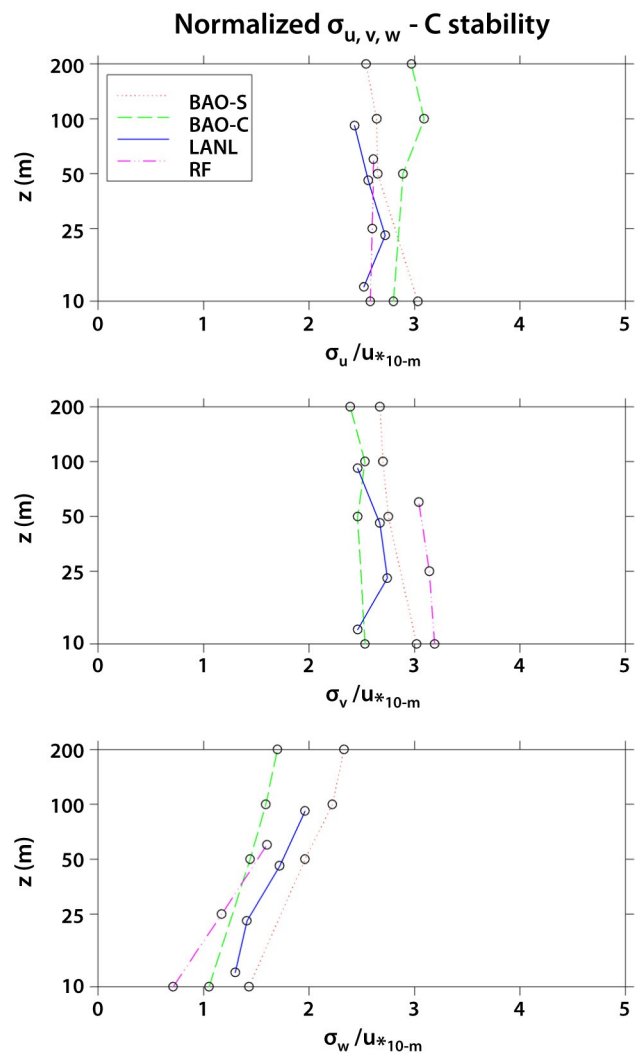


Fig. (4). Same as Fig. (2), except during C stability.

relatively constant with height. All σ_w/u_* profiles agree remarkably well with each other and indicate an increase with height and departure from similarity theory, regardless of fetch.

The σ_u/u_* and σ_v/u_* values increase to between 3 and 5 during F stability and show a tendency to increase with height at the lowest levels as shown in Fig. (7). These σ_w/u_* profiles also show a surprising increase with height for all fetch, with an even greater increase with height than for E stability.

The measured turbulence coefficients exceed widely used values, especially during F stability. For instance, Hanna *et al.* [27] suggest near-surface values of 2.0, 1.3, and 1.3 while Garratt [28] suggests 2.4, 1.9, and 1.25 for $\sigma_{u,v,w}/u_*$, respectively. The differences between these measurements and widely used values increases with height, since the previously mentioned and other studies suggest that normalized turbulence coefficients decrease with height and reach small values at the top of the SBL.

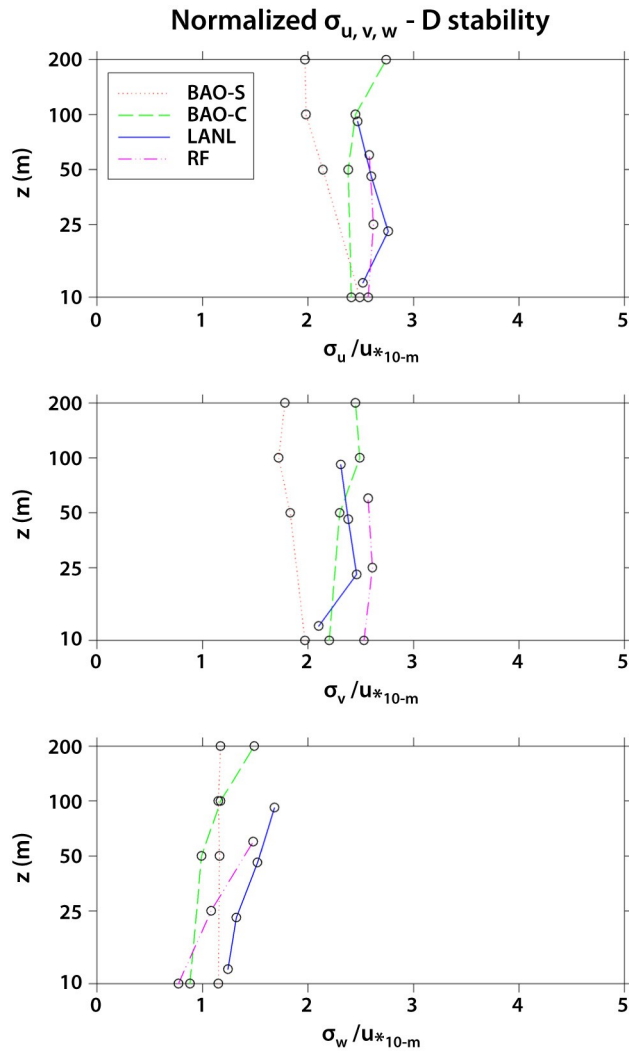


Fig. (5). Same as Fig. (2), except during D stability.

4.3. Comparison of Predicted with Measured-Derived u_*

The turbulence coefficient profiles in the previous section were scaled by *estimated* u_* values based on wind speed, stability, and z_0 because the momentum flux was not measured at the RF tower. Since it is rarely available from routine measurements, the accurate estimation of u_* is important because it often is used to calculate vertical diffusivity profiles in advanced dispersion models or estimate turbulence parameters in simpler models. Therefore, medians of all 15-minute averaged predicted versus measurement-derived u_*

$(\sqrt{-u'w'})$ were calculated for both the simple and complex fetch at BAO and at the LANL for the 6 stability categories and are plotted in Fig. (8).

Results indicate a very good correlation between predicted and measured u_* values, with most differences less than 20%. Large departures of predicted median values (~40%) from measured median values occurred for only two situations: A stability for rough fetch at LANL and D stability for complex fetch at BAO. While the median values show

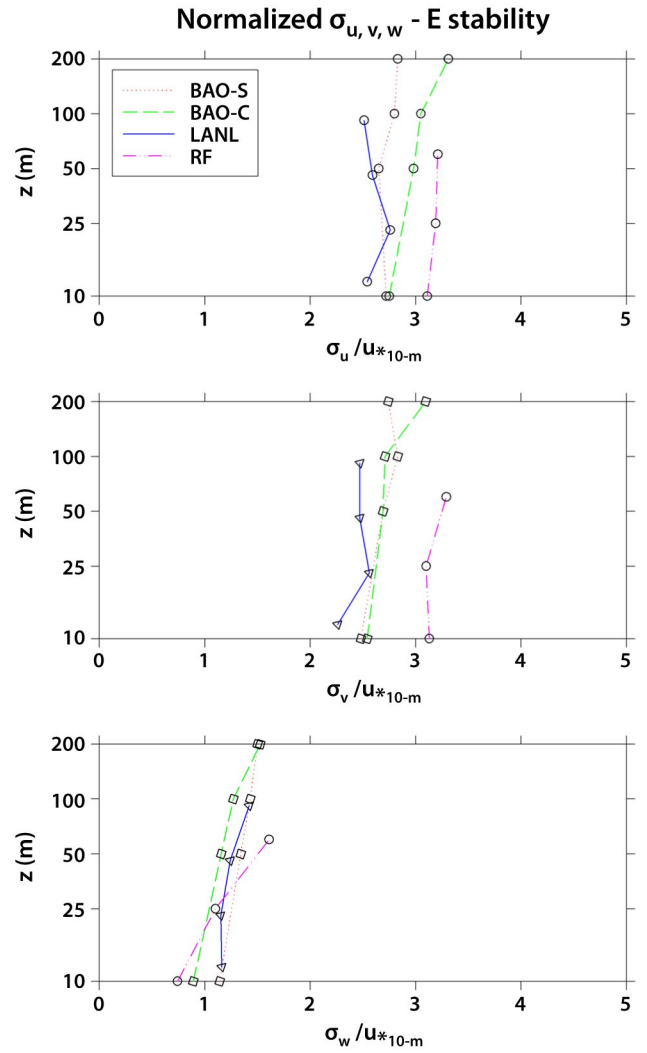


Fig. (6). Same as Fig. (2), except during E stability.

good agreement, there is considerable scatter for individual 15-minute averages. Note that measured median u_* reaches a minimum of about 0.1 ms^{-1} for all fetch during F stability but it reaches a much higher maximum of 0.5 ms^{-1} during C and D stability at LANL, with its larger z_0 because of trees, compared to BAO.

4.4. Angular Wind Direction Fluctuation Standard Deviation Profiles

The standard deviation of angular wind direction fluctuations in the horizontal (σ_θ) and vertical (σ_ϕ) are good indicators of atmospheric dispersive capability and they are often used to determine the dispersion parameters σ_y and σ_z in simple Gaussian models, or they can be used to calculate K_y and K_z in more sophisticated models. Profiles of σ_θ and σ_ϕ for all stabilities were calculated for each fetch and are shown in Figs. (9,10).

The general reduction of σ_θ values as stability increases from A to D stability is similar among all of the fetches.

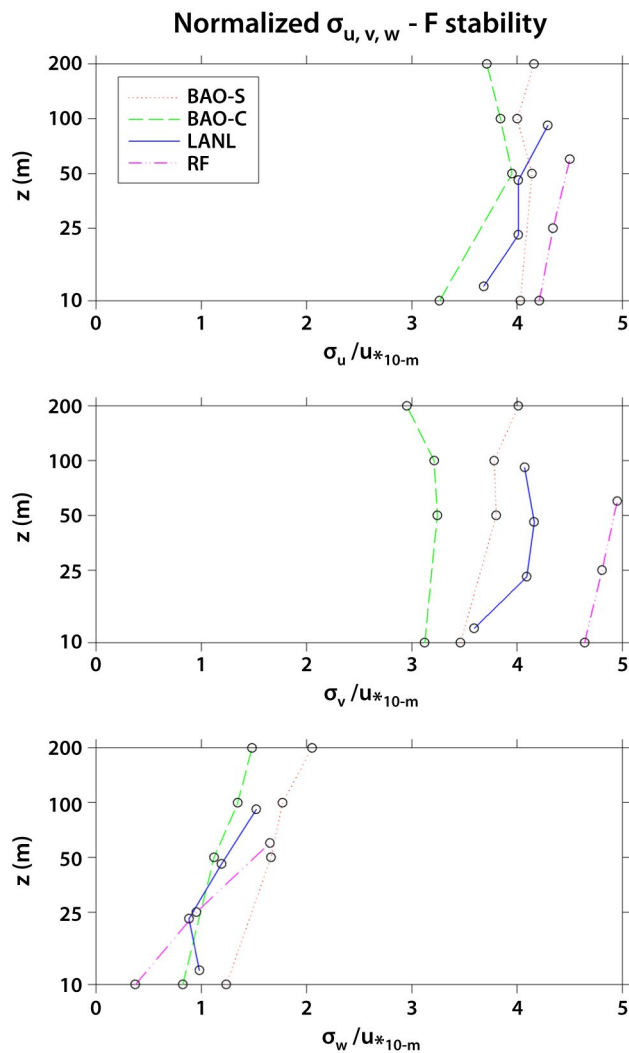


Fig. (7). Same as Fig. (2), except during F stability.

Both the actual values and rate of decrease of σ_θ with height compare reasonably well with widely suggested values [1]. However, median σ_θ values generally increase at several tower levels for all fetch as conditions become stable. This is especially true at BAO for both simple and complex fetch, where σ_θ increases slightly for E stability and then significantly for F stability compared to D stability. The RF site also shows a significant increase in σ_θ for F stability but it shows a very slight incremental decrease from D to E stability. The LANL site shows only a significant increase in σ_θ at the two upper levels during F stability.

The σ_θ profiles also follow expected trends during unstable conditions: the rate of increase with height decreases noticeably as stability increases from A to C stability. Note that the LANL site with nearby trees indicates the largest σ_θ values at lowest heights. However, the σ_θ values show an increase with height during D stability for both the complex BAO and RF fetches instead of an expected decrease (i.e., surface layer similarity and log-law theories assume constant

σ_θ and an increase of wind speed with height). The increase of σ_θ with height does not occur at LANL possibly because the nearby trees generate so much turbulence at the lowest heights.

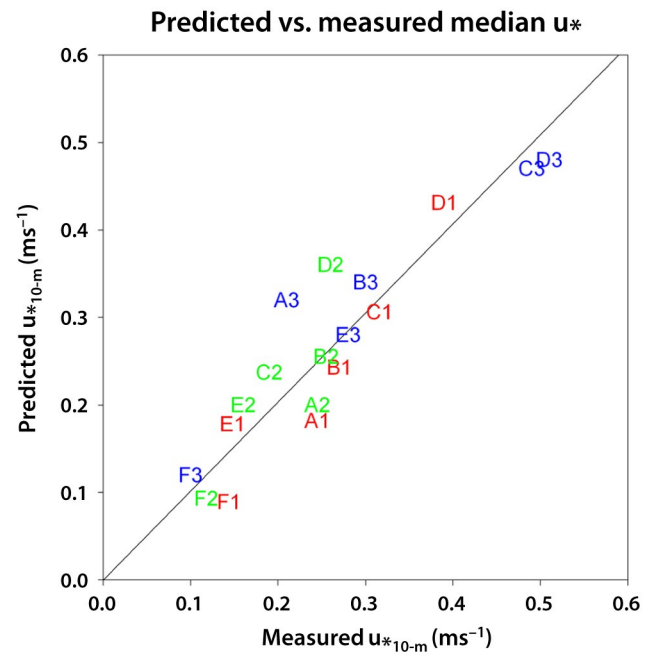


Fig. (8). Scatterplot of medians of 15-minute averaged predicted vs measured u_* values for 3 fetches at 2 sites for 6 stability categories. Symbols denote stability category (A, B, C, etc.) and fetch (1=BAO with simple fetch, 2=BAO with complex fetch, 3=LANL).

The deviation from similarity theory becomes even more noticeable during stable conditions, as σ_θ is relatively constant or it actually increases with height for all fetches. This occurs in spite of the fact that wind speed increases with height for all fetches.

4.5. F Stability Turbulence Coefficient Profiles

The interesting behavior of turbulence during the most stable (F) conditions is further examined by observing the non-normalized turbulence coefficient profiles for only F stability in Fig. (11). Note that the ranges of the median, 10 to 12-m level σ_u and σ_v values are very close to the suggested minimum hourly value for σ_v of 0.5 ms^{-1} suggested by Hanna and Chang [11] and others. Since hourly values are expected to be approximately 30% greater than 15-minute averages, these results are consistent with a minimum hourly value of 0.5 ms^{-1} . A somewhat surprising result is that σ_u and σ_v values have a tendency to remain constant or increase with height for all fetch. Finally, the assumption that σ_u and σ_v values are generally similar to each other in the lowest 100 to 200 m of the SBL also is reasonable.

The σ_w profiles show a dramatic departure from M-O similarity theory, increasing rather than decreasing with

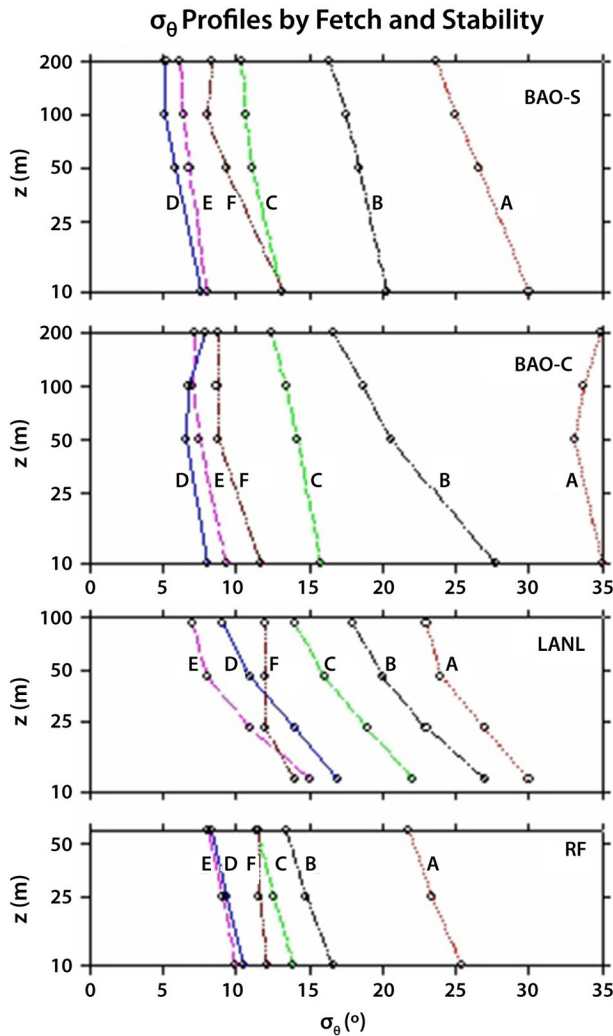


Fig. (9). Measured median σ_θ profiles by fetch and stability. height for all fetch. A composite of all fetches and available heights indicates that σ_w increases from approximately 0.1 to 0.2 ms^{-1} between 10 and 200 m AGL. The long-term increase of median σ_w values for all fetch implies that much of the vertical turbulent energy typically is generated from above as well as from the ground during very stable conditions. Indeed, the increase of σ_w with height may be explained by the generation of intermittent turbulence in the upper part of the NBL not directly related to the surface stress [29]. Nappo [30] suggests that this intermittent turbulence can propagate downward in the form of turbulent bursts.

4.6. Implications for Atmospheric Modeling in SBL

The effect of enhanced vertical turbulence on diffusion in the SBL can be visualized by examining profiles of estimated Kz , an important input to some transport and dispersion models. Similarity theory is widely used to calculate Kz throughout the surface layer by first estimating u_* and L and using a relationship such as the following suggested by Lange [31]:

$$Kz = [0.4 u_* z / \phi_h(z/L)] e^{-4z/h}, \tag{5}$$

where ϕ_h , the dimensionless wind gradient, can be estimated from values suggested by Businger *et al.* [32], for instance.

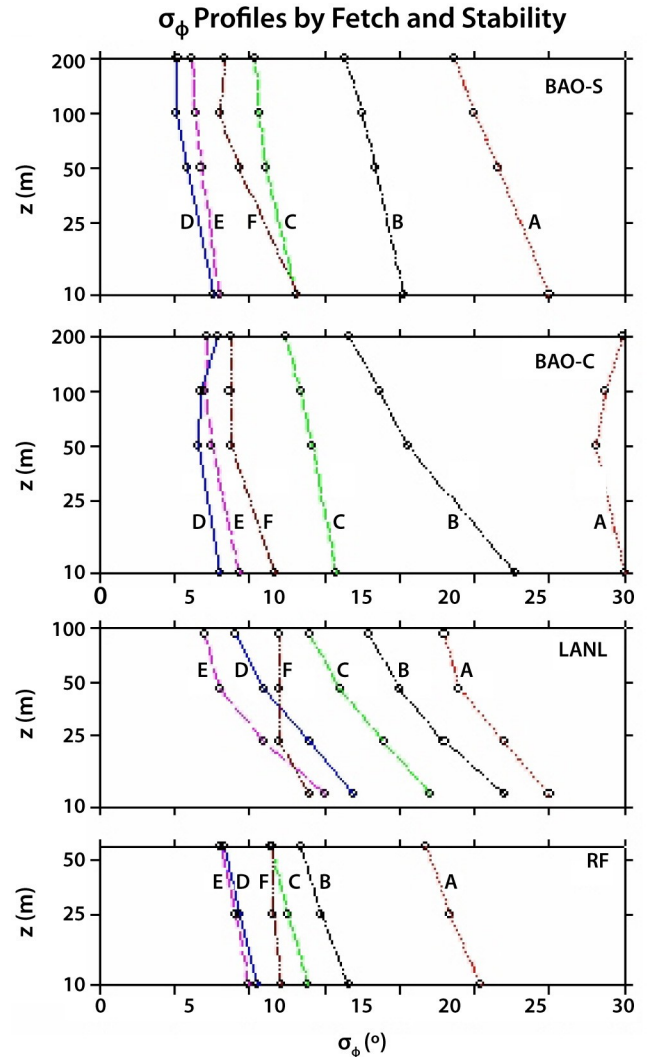


Fig. (10). Measured median σ_ϕ profiles by fetch and stability.

When σ_w measurements are available, Kz can also be calculated from a relationship recommended by Hanna [33]:

$$Kz = A \sigma_w \lambda_{mw}, \tag{6}$$

where Pasquill [7] suggests a value of 0.15 for the constant A and λ_{mw} is the wavelength at which the vertical velocity turbulent kinetic energy peaks. Kaimal and Finnigan [34] suggest the following relationships to estimate λ_{mw} during stable conditions:

$$\lambda_{mw} = z(0.55 + z/L)^{-1}, 0 \leq z \leq L \tag{7}$$

$$\lambda_{mw} = zL(0.45z + 1.1L)^{-1}, L \leq z \leq 2L \tag{8}$$

$$\lambda_{mw} = L, z \geq 2L. \tag{9}$$

Profiles of Kz were calculated at the BAO tower for all fetch using similarity theory (Eq. 5) and measured σ_w (Eq. 6) and are shown in Fig. (12) and Table 2. Note that the value of u_* (0.1 ms^{-1}) used in Eq. 5 is approximately equal to

the measured median value. A typical value of h (500 m) at BAO is estimated from Holzworth [35]. The 25- and 75-percentiles of σ_w -derived Kz values incorporate the variations from only σ_w since $\lambda_{m,w}$ is always specified by Eqs. 7-9. Note the dramatic departure between the two methods to calculate Kz : similarity theory in this case indicates a maximum value at about 20 m while the σ_w method indicates a sharp increase up to about 50 m AGL with less increase above. The σ_w method results in Kz values 1.5 to 16 times larger than those using similarity theory at 10- and 200-m heights (see Table 2), respectively. The variation about the median of σ_w -derived Kz (Fig. 12) indicates skewness toward larger values.

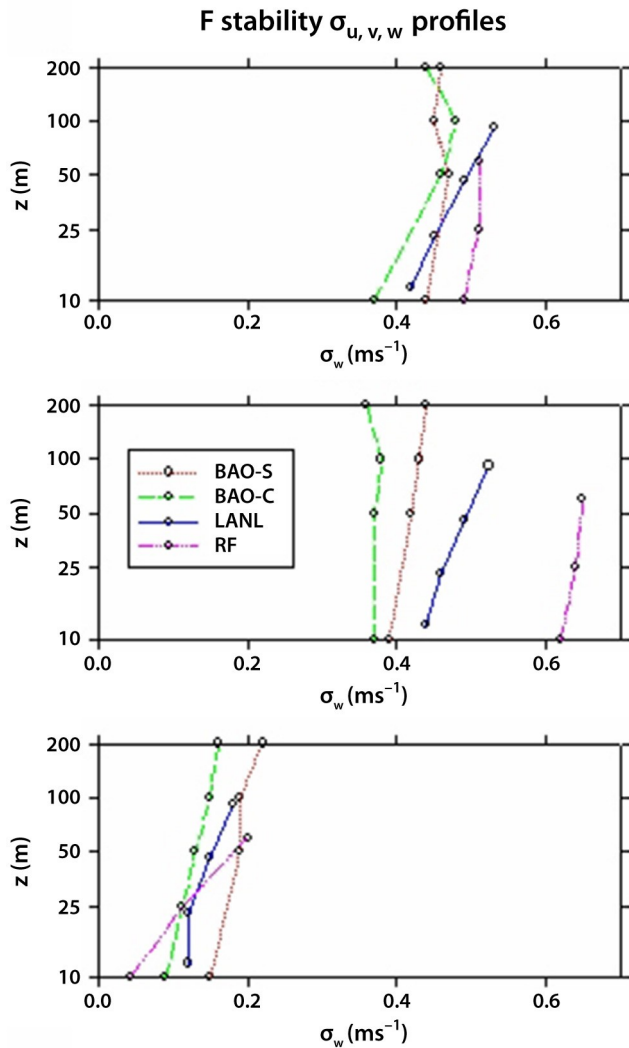


Fig. (11). Turbulence parameter ($\sigma_{u,v,w}$) profiles for 4 fetches at 3 sites during F stability.

The measured σ_w (and estimated Kz) profiles strongly suggest that atmospheric dispersion models that use similarity theory-derived vertical turbulence or diffusivity values may routinely underestimate dispersion in the lowest several hundreds of meters above the ground during very stable conditions, especially farther above the ground. These findings

indicate that ground-level atmospheric concentrations resulting from near ground-level releases will typically be lower than what traditional, similarity-based models indicate. More important, the assumption of similarity theory for slightly elevated releases can potentially cause critical modeling errors, whereby the diffusion of hazardous material to the ground is either underestimated or completely missed. Indeed, a unique dual-tracer field study that took place over a flat, suburban area in Norway illustrates how unexpectedly large turbulence in the SBL can cause large modeling errors during very stable conditions [36]. During weak wind ($< 1 \text{ ms}^{-1}$) occurrences, the use of surface layer theory (wind and temperature profiles) results in ground level concentrations on the order of 5 times greater than measured and predicted concentrations based on turbulence observations up to 500 m downwind of a 1-m AGL release. The use of surface layer theory is similarly inadequate in describing vertical diffusion from the elevated 36-m AGL release: measured and modeled concentrations using turbulence measurements indicate that the plume impacts the ground as close as 100 m downwind. However, the model using surface layer theory shows no ground level concentrations in the first kilometer downwind!

Kz Estimates during Stable Conditions ($h=500 \text{ m}$, $L=20$, $u_*=0.1 \text{ ms}^{-1}$)

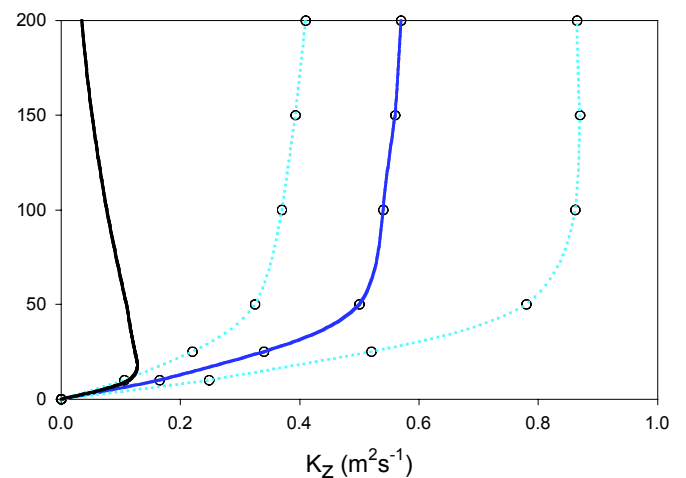


Fig. (12). Estimated median, composite Kz profiles (m^2s^{-1}) at BAO tower during F stability based on measured σ_w (blue) and similarity theory (black). Dashed blue lines indicate 25- and 75-percentile values based on σ_w .

Table 2. Estimated Median, Composite Kz Profiles (m^2s^{-1}) at BAO Tower During F Stability Based on Measured σ_w and Similarity Theory. The Numbers in Parenthesis Represent Variation (25- and 75-Percentile Values) About Median. Assumptions Include Fixed Values of h (500 m), L (20 m), and u_* (0.1 ms^{-1})

z (m)	Kz (σ_w)	Kz (Similarity)	Ratio
200	0.57 (-0.16/+0.30)	0.035	16.3
100	0.54 (-0.17/+0.32)	0.08	7.1
50	0.50 (-0.18/+0.28)	0.11	4.6
10	0.165 (-0.06/+0.08)	0.115	1.45

5. CONCLUSIONS AND RECOMMENDATIONS

Measured long term wind and turbulence parameter profiles up to 200 m AGL and u_* are analyzed in this study for all stability conditions at three, multi-level towers located in the western U.S. Results show that σ_u/u_* , σ_v/u_* , and σ_w/u_* values and profiles for various fetches agree reasonably well with widely used empirical relationships for slightly to strongly unstable conditions, except that σ_v equals or slightly exceeds σ_u . The normalized horizontal coefficients for all fetches also generally agree with the widely used empirical relationships during near-neutral stability. However, σ_w profiles depart from these relationships and similarity theory for three more complex fetches during near-neutral stability as σ_w increases approximately 50 to 100% in the lowest 60 to 200 m. The σ_w values remain nearly constant in the lowest 200 m with simple fetch. The σ_w/u_* values equal approximately one at the 10-m height for both simple and complex fetch. Values of σ_u and σ_v are nearly constant with height for all fetches. The σ_u/u_* and σ_v/u_* values remain relatively constant with height but they increase slightly for slightly stable and then increase to between 3 and 5 for very stable conditions. The σ_w/u_* values show a surprising increase of approximately 50 to 100% in the lowest 100 to 200 m during E and F stability for all fetch, respectively. The 10-m σ_w/u_* values approximately equal one for stable conditions for all fetch. A comparison of predicted and measured u_* values at two of the sites show generally good agreement over 6 stability ranges. Finally, measured σ_w at two of the sites suggest that M-O similarity theory routinely greatly underestimates vertical diffusivity and dispersion during very stable conditions, especially at larger heights, which could thereby lead to large errors in simulated surface concentrations.

Since vertical turbulence is typically not measured routinely on tall towers, and because current ground-based remote sensors are incapable of providing reliable turbulence profiles [37], there is not a large sample with experimental or routine measurements with accurate, deep turbulence profiles. Even though Crescenti [37] indicates that sodar-derived σ_w values show much promise, vertical sodar profiles are often limited in height during neutral and stable conditions.

Based on findings from this study of measurements from tall towers over the western U.S., the following rules of thumb are suggested to describe departure from similarity theory during breezy, near-neutral and stable conditions:

1. For areas in complex terrain or areas up to at least 5 to 10 km or so downwind of sharp terrain rises or dips of 15 to 25 m or so, σ_w/u_* increases by about 50 to 100% in the lowest 60 to 200 m from its approximate value of one at 10 m AGL. Both σ_u/u_* and σ_v/u_* increase with height only slightly and range between 2.5 to 3.5;
2. During stable conditions, σ_u/u_* and σ_v/u_* increase slightly to about 3 during E stability and to between 3

and 5 during F stability, with a tendency to increase slightly with height. The σ_w/u_* values typically increase from approximately one at the 10-m level to about 1.5 and nearly 2 at 200 m AGL for E and F stability, respectively.

3. During F stability, σ_u typically varies between 0.4 to 0.5 ms^{-1} and σ_v typically varies between 0.4 and 0.6 ms^{-1} in the lowest 200 m, with both variables showing a slight tendency to increase with height. The σ_w typically increases from 0.1 to 0.2 ms^{-1} between the 10- and 200-m levels.
4. Since σ_w typically increases in the lowest 200 m, Kz estimated from σ_w is 1.5 to 16 times the value than when similarity theory is assumed. Therefore the use of similarity theory in very stable conditions (e.g., F stability, $L > 0.2$ to 0.4, etc.) in atmospheric dispersion models may cause much too little vertical diffusion in the lowest 200 m or so. This in turn will result in overestimation of near-surface releases and more importantly, often significant *underestimation* of slightly elevated releases.

ACKNOWLEDGEMENTS

I thank the following persons for supplying the data used in this study: Brian Templeman of CIRES, University of Colorado (BAO); Darrell Holt of LANL; and Carey Dickerman of FNMOC, Monterrey, CA (formerly at Rocky Flats Environmental Plant). I appreciate John Nasstrom, Ph.D., of Lawrence Livermore National Laboratory for reviewing this manuscript and making helpful comments. This work was performed under the auspices of the U.S. Department of Energy by the Lawrence Livermore National Laboratory under contract No. W-7405-Eng-48.

REFERENCES

- [1] EPA (U.S. Environmental Protection Agency), Meteorological monitoring guidance for regulatory modeling applications. EPA-454/R-99-005, Office of Air Quality Planning and Standards, Research Triangle Park, NC; 2000.
- [2] Hicks BB. Monin-Obukhov similarity—An historical perspective. Eleventh Symposium on Boundary Layers and Turbulence, Charlotte, NC. Am Meteor Soc 1995; 1-4.
- [3] Panofsky HA, Egolf CA, Lipschutz R. On characteristics of wind direction fluctuations in the surface layer. Bound Layer Met 1978; 15: 439-46.
- [4] Hanna SR. Measured σ_v and σ_θ in complex terrain near the TVA Widows Creek. Alabama Steam Plant. Atmos Environ 1980; 14: 401-7.
- [5] Ludwig FL, Dabberdt WF. Comparison of two practical atmospheric stability classification schemes in an urban atmosphere. J Appl Meteor 1976; 15: 1172-6.
- [6] Tieleman HW. Wind characteristics in the surface layer over heterogeneous terrain. J Wind Eng Ind Aerodyn 1992; 1: 329-40.
- [7] Pasquill F. Atmospheric Diffusion, 2nd Ed. John Wiley and Sons, 1974; 429 pp. (see page 77).
- [8] Beljaars ACM, Schotanus P, Nieuwstadt FTM. Surface layer similarity under nonuniform fetch conditions. J Clim Appl Meteor 1983; 22: 800-1810.
- [9] Bowen BM. Neutral surface layer turbulence over complex terrain. Ninth Joint Conf. on the Applications of Air Pollution Meteorology, Atlanta, GA. Am Meteor Soc 1996; 411-416.
- [10] Bowen BM. Near-neutral surface layer turbulence at the Boulder atmospheric observatory tower. J Appl Meteor 2000; 39: 716-24.

- [11] Hanna SR, Chang JC. Boundary-layer parameterizations for applied dispersion modeling over urban areas. *Bound Layer Met* 1992; 58: 229-59.
- [12] Weber AH, Kurzeja RJ. Nocturnal planetary boundary layer structure and turbulence episodes during the Project STABLE field program. *J Appl Meteor* 1991; 30: 1117-33.
- [13] Banta RM, Olivier LD, Gudiksen PH. Implications of small-scale flow features to modeling dispersion over complex terrain. *J Appl Meteor* 1995; 35: 330-42.
- [14] Schotz S, Panofsky HA. Wind characteristics at the Boulder Atmospheric Observatory. *Bound-Layer Met* 1980; 17: 333-51.
- [15] Crescenti GH. Development of quality assurance and quality control guidance for ground-based remote sensors for use in regulatory modeling. Ninth Joint Conf. on the Applications of Air Pollution Meteorology, Atlanta, GA. *Am Meteor Soc* 1996; 551-55.
- [16] Sedefian L, Bennett E. A comparison of turbulence classification schemes. *Atmos Environ* 1980; 14: 741-50.
- [17] Businger JA. Turbulent transfer in the atmospheric surface layer. Workshop on Micrometeorology. *Amer Meteor Soc* 1973; pp. 67-120.
- [18] Holtslag AAM, Van Ulden AP. A simple scheme for daytime estimates of the surface fluxes from routine weather data. *J Clim Appl Meteor* 1983; 22: 517-29.
- [19] Dyer AJ. A review of flux-profile relationships. *Bound-Layer Met* 1974; 7: 363-72.
- [20] Paulson CA. The mathematical representation of wind speed and temperature profiles in the unstable atmospheric surface layer. *J Appl Meteor* 1970; 9: 856-61.
- [21] Arya SP. *Air Pollution Meteorology and Dispersion*. Oxford University Press, 1999. 310 pp. (see Chapter 4).
- [22] Golder D. Relations among stability parameters in the surface layer. *Bound Layer Met* 1972; 3: 47-58.
- [23] Verkaik JW, Holtslag AAM. Wind profiles, momentum fluxes and roughness lengths. *Bound Layer Met* 2007; 122: 701-19.
- [24] Gryning SE, Batchvarova E, Brummer B, Jorgensen H, Larsen S. *Bound-Layer Met* 1972; 24: 251-68.
- [25] Tieleman HW. Stong wind observations in the atmospheric surface layer. *J Wind Eng Ind Aerodyn* 2008; 96: 41-77.
- [26] Panofsky HA, Tennekes H, Lenschow DH, Wyngaard JC. The characteristics of turbulent velocity components in the surface layer under convective conditions. *Bound Layer Met* 1977; 11: 355-61.
- [27] Hanna SR, Briggs GA, Hosker RP. Handbook on atmospheric diffusion. U.S. Dept. of Energy Report DOE/TIC-11223, 102 pp. [Available from NTIS, U.S. Dept. of Commerce, Springfield, VA 21161.] 1982.
- [28] Garratt JR. *The atmospheric boundary layer*. Cambridge University Press, 1992; pp. 316.
- [29] Mahrt L. Vertical structure and turbulence in the very stable boundary layer. *J Atmos Sci* 1985; 42: 2333-49.
- [30] Nappo CJ. Sporadic breakdowns of stability in the PBL over simple and complex terrain. *Bound Layer Met* 1991; 54: 69-87.
- [31] Lange R. Transferability of a three-dimensional air quality model between two different sites in complex terrain. *J Appl Meteor* 1989; 28: 665-79.
- [32] Businger JA, Wyngaard JC, Izumi Y, Bradley EF. Flux-profile relationships in the atmospheric surface layer. *J Atmos Sci* 1971; 28: 181-9.
- [33] Hanna SR. A method of estimating vertical eddy transport in the planetary boundary layer. *J Atmos Sci* 1968; 25: 1026.
- [34] Kaimal JC, Finnigan JJ. *Atmospheric Boundary Layer Flows*. Oxford University Press, 1994; pp. 289 (see Chapter 2).
- [35] Holzworth GC. Mixing heights, wind speeds, and potential for urban air pollution throughout the contiguous United States. U.S. Environmental Protection Agency Office of Air Programs Publication No. AP-101, 118 pp. [Available from Superintendent of Documents, U.S. Govt. Printing Office, Washington, D.C. 20402] 1972.
- [36] Gronskei KE. Variation in dispersion conditions with height over urban areas - results of dual tracer experiments. Preprints, Ninth Symposium on Turbulence and Diffusion, Roskilde, Denmark, *Am Meteor Soc* 1990; 297-300.
- [37] Crescenti GH. A look back on two decades of Doppler sodar comparison studies. *Bull Amer Soc* 1997; 78: 651-73.

Received: March 27, 2008

Revised: April 15, 2008

Accepted: May 2, 2008

© Brent M. Bowen; Licensee *Bentham Open*.This is an open access article distributed under the terms of the Creative Commons Attribution License (<http://creativecommons.org/licenses/by/2.5/>), which permits unrestricted use, distribution, and reproduction in any medium, provided the original work is properly cited.